Inorg. Chem. **2002**, *41*, 6404–6411

Di-*tert*-butyl Phosphate as Synthon for Metal Phosphate Materials via Single-Source Coordination Polymers $[M(dtbp)_2]_n$ (M = Mn, Cu) and $[Cd(dtbp)_2(H_2O)]_n$ (dtbp-H = $(tBuO)_2P(O)OH$)†

Malaichamy Sathiyendiran and Ramaswamy Murugavel*

Department of Chemistry, Indian Institute of Technology-Bombay, Powai, Mumbai-400 076, India

Received August 26, 2002

Reaction of $M(OAc)_2 \cdot xH_2O$ (M = Mn, Cu, or Cd) with di-*tert*-butyl phosphate (dtbp-H) in a 1:2 molar ratio in methanol followed by slow crystallization of the resultant solid in MeOH/THF medium results in the formation of three new polymeric metal phosphates $[M(dtbp)_2]_n$ [M = Mn, **1** (beige); M = Cu, **2** (blue)] and $[Cd(dtbp)_2(H_2O)]_n$, **3** (colorless)] in good yields. The formation of $[Mn(dtbp)_2]_n$ (**1**) proceeds via tetrameric manganese phosphate $[Mn_4(O)(dtbp)_6]$ (**4**), which has been isolated in an analytically pure form. Perfectly air- and moisture-stable compounds **1**–**4** were characterized with the aid of analytical, thermoanalytical, and spectroscopic techniques. The molecular structures of **1**–**3** were further established by single-crystal X-ray diffraction studies. Crystal data for **1**: $C_{32}H_{72}Mn_2O_{16}P_4$, monoclinic, $P2_1/c$, $a = 19.957(4)$ Å, $b = 13.419(1)$ Å, $c = 18.083(2)$ Å, $\beta = 91.25(2)°$, $Z = 4$. Crystal data for **2**: $C_{16}H_{36}CuO_8P_2$, orthorhombic, *Pccn*, $a = 23.777(2)$ Å, $b = 10.074(1)$ Å, $c = 10.090(1)$ Å, $Z = 4$. Crystal data for **3**: $C_{48}H_{114}Cd_3O_{27}P_6$, triclinic, $P\bar{1}$, $a = 12.689(3)$ Å, $b = 14.364(3)$ Å, $c = 22.491(5)$ Å, $\alpha = 84.54(3)°$, $\beta = 79.43(3)°$, $\gamma = 70.03(3)°$, $Z = 2$. The diffraction studies reveal three different structural forms for the three compounds investigated, each possessing a one-dimensional coordination polymeric structure. While alternating triple and single dtbp bridges are found between the adjacent Mn^{2+} ions in **1**, uniform double dtbp bridges across the adjacent Cu^{2+} ions are present in **2**. The cadmium ions in the structure of **3** are pentacoordinated. Thermal analysis (TGA and DSC) indicates that compounds **1**–**3** convert to the corresponding crystalline metaphosphate materials $M(PO_3)_2$, in each case at temperatures below 500 °C. Similarly, the thermal decomposition of **4** results in the formation of $Mn(PO_3)_3$ and $Mn_2P_2O_7$. The final materials obtained by independent thermal decomposition of bulk samples have been characterized using IR spectroscopic, powder diffraction, and N_2 adsorption studies.

Introduction

There have been several efforts in recent years to synthesize soluble molecular cage-like metallasilicates and phosphates in order to understand the local structures of complex silicate and phosphate materials. In particular, recent studies on metal-containing molecular siloxanes, phosphonates, and phosphates have opened up new possibilities in assembling inorganic clusters incorporating Si−O−M and P−O−M linkages.[1−14] These molecular cluster compounds, apart from modeling the local structures of silicate and phosphate materials, can also be used as single-source precursors for the eventual preparation of advanced materials by employing processes such as sol−gel routes.[15,16] Although

* Corresponding author. E-mail: rmv@iitb.ac.in. Fax: +(22) 2572 3480. Phone: +(22) 2576 7163.

† This paper is dedicated to Professor Animesh Chakravorty.

(1) Murugavel, R.; Chandrasekhar, V.; Roesky, H. W. *Acc. Chem. Res.* **1996**, *29*, 183.
(2) Murugavel, R.; Voigt, A.; Walawalkar, M. G.; Roesky, H. W. *Chem. Rev.* **1996**, *96*, 2205.
(3) Walawalkar, M. G.; Roesky, H. W.; Murugavel, R. *Acc. Chem. Res.* **1999**, *32*, 117.
(4) Murugavel, R.; Prabusankar, G.; Walawalkar, M. G. *Inorg. Chem.* **2001**, *40*, 1084.
(5) Murugavel, R.; Walawalkar, M. G.; Prabusankar, G.; Davis, P. *Organometallics* **2001**, *20*, 2639.
(6) Murugavel, R.; Shete, V. S.; Baheti, K.; Davis, P. *J. Organomet. Chem.* **2001**, *625*, 195.
(7) Murugavel, R.; Sathiyendiran, M.; Walawalkar, M. G. *Inorg. Chem.* **2001**, *40*, 427.
(8) Murugavel, R.; Sathiyendiran, M. *Chem. Lett.* **2001**, 84.
(9) Chandrasekhar, V.; Kingsley, S.; Rhatigan, B.; Lam, M. K.; Rheingold, A. L. *Inorg. Chem.* **2002**, *41*, 1030.
(10) Lugmair, C. G.; Fujdala, K. L.; Tilley, T. D. *Chem. Mater.* **2002**, *14*, 888.
(11) Feher, F. J.; Budzichowski, T. A. *Polyhedron* **1995**, *14*, 3239.
(12) King, L.; Sullivan, A. C. *Coord. Chem. Rev.* **1999**, *189*, 19.

10.1021/ic0259787 CCC: $22.00
Published on Web 11/05/2002

Chart 1. Discrete Metal Di-*tert*-butyl Phosphate Complexes

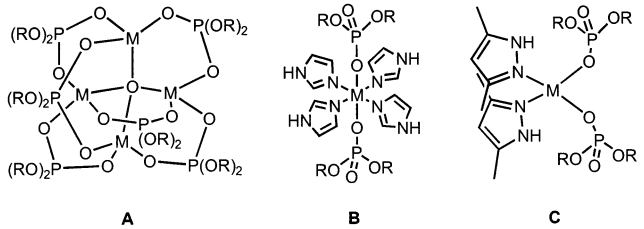

the early applications of sol−gel science were on the use of metal alkoxides as precursors for glasses and similar ceramic materials,[15] later years saw the extension of this process for the preparation of several metal silicate and phosphate assemblies.[16] The most appealing advantage of employing a single-source molecular precursor approach is its ability to provide atomic level control over a material's composition and homogeneity.[17]

After the success of the sol−gel process for the preparation of new materials and the synthesis of model compounds for silicate and phosphate materials, low-temperature thermolysis of single source molecular precursors for the preparation of advanced materials is gaining considerable attention owing to its ability to provide atomic level control over the composition and homogeneity of the final materials. Recent work has shown that tri-*tert*-butoxysilanol [(*t*BuO)$_3$Si(OH)] and di-*tert*-butyl phosphate [(*t*BuO)$_2$P(O)OH] (dtbp-H) could serve as ideal starting materials for the preparation of metal complexes which decompose neatly at low temperatures to yield, respectively, fine particle metal silicates or phosphates.[7,8,18−20]

The use of dtbp-H to prepare precursors **A**−**C** and their conversion into phosphate materials have been recently reported by us (Chart 1).[7,8] Although these molecules are excellent precursors for low-temperature pyrolysis, the decomposition of **A** leads to a mixture of meta- and pyrophosphates, while the decomposition of **B** or **C** results in the contamination of the final material with nitrogen impurities.[7] Hence, molecular precursors with a strict 1:2 or 1:1 M/dtbp ratio and the exclusion of auxiliary ligands are highly desired for the preparation of high purity phosphate materials. Careful monitoring of the reaction conditions and screening of a variety of solvents by us have now resulted in the preparation of a series of new polymeric metal phosphate precursors with a 1:2 M/dtbp ratio. The results of this investigation along with X-ray structure elucidation of three new polymeric phosphates, their characterization data, and their solid state thermolysis to yield high purity M(PO$_3$)$_2$ materials are reported in this paper.

Experimental Section

Instruments and Methods. Because all the starting materials and the products reported in this study were found to be stable toward moisture and air, no specific precautions were taken to rigorously exclude air although all manipulations were routinely carried out on a vacuum line. Elemental analyses were performed on a Carlo Erba (Italy) Model 1106 elemental analyzer. Infrared spectra were recorded on a Nicolet Impact 400 spectrometer using KBr diluted pellets. TGA and DSC measurements were carried out at RSIC, IIT-Bombay, on a DuPont thermal analyzer model 2100 under a stream of nitrogen gas and at a heating rate of 10 °C/min. The powder XRD measurements were obtained on a PW1729 X-ray generator. Surface area and porosity measurements of the metal phosphate materials were carried out by N_2 adsorption studies on a Quantochrome Autosorb-1C chemisorption−physisorption analyzer.

Solvents and Starting Materials. Commercial grade solvents were purified by conventional procedures and were distilled prior to their use. Starting materials such as metal acetates were procured from commercial sources and used as received. Di-*tert*-butyl phosphate (dtbp-H) was synthesized from di-*tert*-butyl phosphite using a previously reported procedure.[21] Owing to its thermal instability, dtbp-H was freshly prepared by acid hydrolysis from its potassium salt prior to its use.

Synthesis of [Mn(dtbp)$_2$]$_n$ (1). A solution of Mn(OAc)$_2$·4H$_2$O (0.122 g, 0.5 mmol) in MeOH (25 mL) was added to a solution of dtbp-H (0.210 g, 1 mmol) in MeOH (20 mL) with constant stirring. To the resulting solution in a small beaker was added 2,6-dimethylpyridine (0.1 mL) slowly along the walls, and this was left for crystallization. Crystals formed after 4 days were removed by filtration and air-dried. Yield: 0.185 g (79%). Anal. Calcd for C$_{16}$H$_{36}$MnO$_8$P$_2$: C, 40.60; H, 7.67. Found: C, 40.60; H, 7.90. IR data (KBr): 2983(vs), 2936(vs), 1544(s), 1478(m), 1395(s), 1369(s), 1262(vs), 1184(vs), 1087(vs), 1040(vs), 1006(vs), 917(s), 838(s), 819(s), 819(s), 725(s), 709(s), 593(s), 551(s), 507(s) cm^{-1}. UV−vis (MeOH): 300 nm.

Synthesis of [Cu(dtbp)$_2$]$_n$ (2). A solution of Cu(OAc)$_2$·H$_2$O (0.199 g, 1 mmol) in MeOH (25 mL) was added to a solution of dtbp-H (0.420 g, 2 mmol) in MeOH (20 mL) with constant stirring. The clear solution obtained was allowed to reflux over 12 h and filtered. The solvent was removed under vacuum, and the precipitate obtained was washed with pentane and air-dried. The product was crystallized from a methanol/THF mixture (50 mL/5 mL). Yield: 0.31 g (64%). Anal. Calcd for C$_{16}$H$_{36}$CuO$_8$P$_2$: C, 39.87; H, 7.53. Found: C, 39.71; H, 7.94. IR data (KBr): 2986(vs), 2935(vs), 1488(m), 1395(s), 1371(s), 1245(vs), 1204(s), 1178(vs), 1102(vs), 1072-

(13) (a) Lorenz, V.; Fischer, A.; Giessmann, S.; Gilje, J. W.; Gun'ko, Y.; Jacob, K.; Edelmann, F. T. *Coord. Chem. Rev.* **2000**, *206-207*, 321. (b) Mason, M. *J. Cluster Sci.* **1998**, *9*, 1.
(14) Pahari-Dutta, D.; Jain, V. K. *Phosphorus, Sulfur Silicon Relat. Elem.* **2000**, *166*, 15.
(15) (a) Brinker, C. J.; Scherer, G. W. *Sol-Gel Science*; Academic Press: Boston, 1990. (b) *Sol-Gel Technology for Thin Films, Fibres, Preforms, Electronics, and Speciality Shapes*; Klein, L. C., Ed.; Noyes Publishers: Parkridge, NJ, 1988. (c) Corriu, R. J. P.; Leclercq, D. *Angew. Chem., Int. Ed. Engl.* **1996**, *35*, 1421. (d) Mehrotra, R. C. *J. Non-Cryst. Solids* **1996**, *121*, 1. (e) www.solgel.com.
(16) (a) Che, M.; Cheng, Z. X.; Louis, C. *J. Am. Chem. Soc.* **1995**, *117*, 208. (b) Mostafa, M. R.; Youssef, A. M. *Mater. Lett.* **1998**, *34*, 405. (c) Harmer, M. A.; Vega, A. J.; Flippen, R. B. *Chem. Mater.* **1994**, *6*, 1903.
(17) (a) Williams, A. G.; Interrante, L. V. In *Better Ceramics Through Chemistry*; Brinker, C. J., Clark, D. E., Ulrich, D. R., Eds.; Materials Research Society Symposia Proceedings; North-Holland Publishers: New York, 1984; Vol. 32. (b) Chandler, C. D.; Roger, C.; Hampden-Smith, M. J. *Chem. Rev.* **1993**, *93*, 1205. (c) *Organosilicon Chemistry III: From Molecules to Materials*; Auner, N., Weis, J., Eds.; Wiley-VCH: Weinheim, 1998.
(18) (a) Fujdala, K. L.; Tilley, T. D. *Chem. Mater.* **2002**, *14*, 1376. (b) Fujdala, K. L.; Tilley, T. D. *J. Am. Chem. Soc.* **2001**, *123*; 10133. (c) Fujdala, K. L.; Tilley, T. D. *Chem. Mater.* **2001**, *13*, 2683. (d) Rulkens, R.; Male, J. L.; Terry, K. W.; Olthof, B.; Khodakov, A.; Bell, A. T.; Iglesia, E.; Tilley, T. D. *Chem. Mater.* **1999**, *11*, 2966.
(19) (a) Lugmair, C. G.; Tilley, T. D.; Rheingold, A. L. *Chem. Mater.* **1997**, *9*, 339. (b) Lugmair, C. G.; Tilley, T. D. *Inorg. Chem.* **1998**, *37*, 1821.
(20) Lugmair, C. G.; Tilley, T. D.; Rheingold, A. L. *Chem. Mater.* **1999**, *11*, 1615.
(21) Zwierzak, A.; Kluba, M. *Tetrahedron* **1971**, *27*, 3163.

(vs), 1002(vs), 923(s), 894(s), 827(s), 704(s), 616(s) cm^{-1}. UV−vis (MeOH): 300, 800 nm.

Synthesis of $[Cd(dtbp)_2(H_2O)]_n$ (3). Solid dtbp-H (2.10 g, 10 mmol) was added to a solution of cadmium acetate (1.24 g, 5 mmol) in methanol (50 mL), and the resulting solution was stirred for 12 h and then allowed to stand at room temperature. White layered crystals were obtained from this solution in 7 days. Single crystals suitable for X-ray measurements were obtained by repeated recrystallization from a methanol/THF/benzene (20/5/3 mL) solution. Yield: 1.8 g (66%). Anal. Calcd for $C_{16}H_{38}CdO_9P_2$: C, 35.01; H, 6.98. Found: C, 34.58; H, 6.54. IR data (KBr): 3590 (b), 2973(vs), 2934(s), 1565(s), 1427(s), 1381(s), 1262(s), 1183(vs), 1090(s), 992(vs), 927(m), 841(s), 723(s), 597(s), 519(s) cm^{-1}. ^1H NMR (CH_3OD, 300 MHz): δ 1.38 (s, *t*Bu). ^{31}P NMR (CH_3OD, 122 MHz): δ 7.7. UV−vis (MeOH): 290 nm.

Synthesis of $[Mn_4(\mu_4\text{-}O)(dtbp)_6]$ (4). A solution of $Mn(OAc)_2 \cdot 4H_2O$ (0.245 g, 1 mmol) in MeOH (25 mL) was added to a solution of dtbp-H (0.315 g, 1.5 mmol) in MeOH (20 mL) with constant stirring. The resultant solution was filtered and left in a beaker. Crystals of **4** formed after 2 days were removed by filtration and dried. Yield: 185 mg (50%). Anal. Calcd for $C_{48}H_{108}Mn_4O_{25}P_6$: C, 38.66; H, 7.30. Found: C, 37.48; H, 7.38. IR data (KBr): 2986(vs), 2933(vs), 1477(m), 1393(s), 1368(s), 1249(vs), 1179(vs), 1078(vs), 1039(vs), 993(vs), 916(s), 832(s), 709(s), 595(s), 550(s), 507(s) cm^{-1}. Dissolution of **4** in a methanol/THF mixture (4:1) followed by slow crystallization results in quantitative formation of **1**.

Decomposition of 1−3. Using the TGA data on samples **1**−**3**, the thermal decomposition studies of the bulk samples were carried out on a temperature-controlled furnace. In a typical experiment, 2 g of the respective sample was placed on a alumina boat and heated in air initially at 200 °C for 48 h. After removing an adequate amount of the resultant pyrolyzed solid (ca. 300 mg) for spectral analysis, the solid was successively heated at temperatures 300, 350, 400, 500, and 600 °C after removing samples at each stage for characterization. The samples collected at each stage were characterized by IR spectroscopy, PXRD, and N_2 adsoprtion studies.

X-ray Structure Analysis. Single crystals of **1**−**3** suitable for X-ray structure analysis were grown by using the procedures described vide supra. Single-crystal X-ray diffraction measurements for **1** and **3** were obtained on a Siemens STOE AED2 diffractometer at 150° K while the data for **2** were obtained on a Nonius MACH3 diffractometer at 293° K. In each case, unit cell dimensions were determined using 25 or more well-centered and well-separated strong reflections. The intensity data were corrected for Lorentz and polarization effects. The structure solutions for all three compounds were achieved using direct methods (SHELXS-97),[22a] and the structures were refined using SHELXL-97.[22b] The positions of hydrogen atoms were geometrically fixed and refined using a riding model. All non-hydrogen atoms were refined anisotropically. Other details pertaining to data collection, structure solution, and refinement are given in Table 1. Atomic coordinates, complete bond distances and bond angles, and anisotropic thermal parameters of all non-hydrogen atoms for all three compounds are available as Supporting Information.

Results and Discussion

Synthesis and Spectra. The synthetic procedure used for the preparation of the new coordination polymers **1**−**3** is shown in Scheme 1. While the coordination polymers $[Cu(dtbp)_2]_n$ (**2**) and $[Cd(dtbp)_2(H_2O)]_n$ (**3**) are accessible as crystalline solids in moderate yields from the respective metal acetates and dtbp-H in methanol, the direct reaction of manganese acetate with dtbp-H in methanol medium initially yielded the tetrameric manganese phosphate $[Mn_4(\mu_4\text{-}O)(dtbp)_6]$ (**4**). Addition of a base such as pyridine, 2,6-dimethylpyridine, pyrazine, 2-hydroxypyridine, and 3,5-dimethylpyrazole-1-ethanol, to this reaction mixture, however, leads to the quantitative conversion of **4** to $[Mn(dtbp)_2]_n$ (**1**).

Polymer **1** can also be obtained by simply crystallizing pure tetramer **4** in the presence of any added amine. In this context, it is interesting to note that the analogous zinc tetramer $[Zn_4(\mu\text{-}O)(dtbp)_6]$, recently reported by Tilley et al.,[19] also rearranges to the polymeric structure $[Zn_2(dtbp)_2]_n$, but in the presence of an acid and not a base. Thus, the role of the added base was evaluated by an independent reaction of the starting materials in a reaction medium of methanol containing THF. As expected, the only isolated product was **1**, clearly indicating that use of a mild base such as THF is

Table 1. Crystal Data and Details of Structure Determination of **1**−**3**

	1	**2**	**3**
empirical formula	$C_{32}H_{72}Mn_2O_{16}P_4$	$C_{16}H_{36}CuO_8P_2$	$C_{48}H_{114}Cd_3O_{27}P_6$
fw	946.66	481.93	1646.4
T, K	203(2)	293(2)	203(2)
wavelength	0.710 73 Å	0.710 73 Å	0.710 73 Å
cryst syst	monoclinic	orthorhombic	triclinic
space group	$P2_1/c$	*Pccn*	$P\bar{1}$
a, Å	19.957(4)	23.777(2)	12.689(3)
b, Å	13.419(3)	10.074(1)	14.364(3)
c, Å	18.083(2)	10.090(1)	22.491(5)
α, deg			84.54(3)
β, deg	91.25(2)		79.43(3)
γ, deg			70.03(3)
V, Å^3; *Z*	4841.7(1); 4	2416.8(5); 4	3785(1); 2
ρ(calcd), g cm^{-3}	1.299	1.324	1.445
μ, mm^{-1}	0.712	1.070	1.030
R1, wR2[a] $[I > 2\sigma(I)]$	0.052; 0.122	0.062; 0.167	0.038; 0.081
R1, wR2 (all data)	0.067; 0.134	0.093; 0.180	0.050; 0.089
GOF	1.043	1.079	1.053

[a] $R1 = ||F_o| - |F_c||/|F_o|$; $wR2 = \{[w(F_o^2 - F_c^2)^2]/[w(F_o^2)^2]\}^{1/2}$.

Scheme 1. Synthesis of **1**−**4**

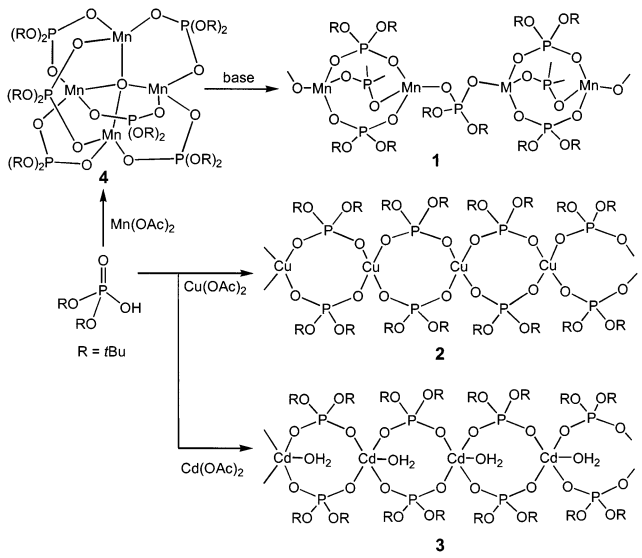

(22) (a) Sheldrick, G. M. *SHELXS-97: Program for Crystal Structure Solution*; University of Göttingen: Göttingen, Germany, 1997. (b) Sheldrick, G. M. *SHELXL-97: Program for Crystal Structure Refinement*; University of Göttingen: Göttingen, Germany, 1997.

necessary in the reaction medium for the formation of **1** directly from the metal acetate and dtbp-H. Similarly, addition of small amounts of THF during crystallization also results in the increased yields of copper and cadmium polymers **2** and **3**.[23] Hence, it appears that the formation of all the three polymers is greatly facilitated by the addition of a weak Lewis base.

Compounds **1**−**4** have been characterized by analytical, spectroscopic, and thermoanalytical techniques. The crystallized products were analytically pure. Although the analytical data for the compounds yielded simple molecular formulas of $[M(dtbp)_2]$ for **1** and **2** and $[M(dtbp)_2(H_2O)]$ for **3**, the monomeric form for these compounds is ruled out because of the well-known inability of dtbp or any phosphate group to chelate to the metal ions.[24] Hence, it is likely that these compounds exist in a polymeric or oligomeric form as is often observed in metal phosphinate chemistry.[25−28] On the other hand, the analytical data obtained for **4** correspond to the $[Mn_4(\mu_4\text{-O})(dtbp)_6]$ formulation which is similar to that of beryllium acetate or a basic zinc acetate structure with a μ_4-O ligand. Such structures for metal di-*tert*-butyl phoshate complexes have been recently reported by Tilley and us in the case of cobalt and zinc metals.

The IR spectra show strong bands at 1185, 1090, and 1005 cm^{-1} for **1** and at 1178, 1072, and 998 cm^{-1} for **2** which are assigned to the antisymmetric and symmetric O−P−O, and M−O−P stretching frequencies, respectively. In addition to these bands, cadmium polymer **3** also shows a strong and broad absorption at 3590 cm^{-1} corresponding to the O−H stretching of the coordinated water molecule. The ^1H NMR spectrum of **3** shows a single signal at δ 1.38 ppm corresponding to the CH_3 protons of the *t*Bu group. The ^{31}P NMR spectrum also shows a single resonance at δ 7.7 ppm suggesting only one environment for the dtbp ligand in **3** in solution. The UV−vis spectra of all the three products showed an absorption maximum in the UV region at around 300 nm; an additional broad absorption maximum at 800 nm was observed for **2**.

Molecular Structures. To clearly establish the structure and the degree of association of metal centers, a single-crystal X-ray diffraction study was carried out for compounds **1**−**3**.[29] Interestingly, the results reveal three different structural forms for the three compounds studied, each possessing a polymeric

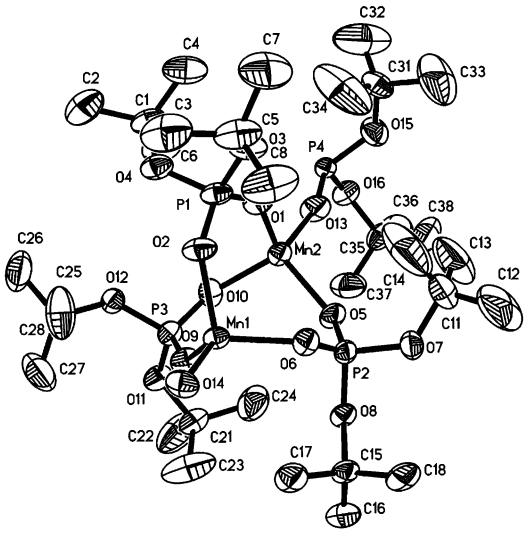

Figure 1. ORTEP (50% probability level) of the asymmetric part in the unit cell in $[Mn(dtbp)_2]_n$ (**1**).

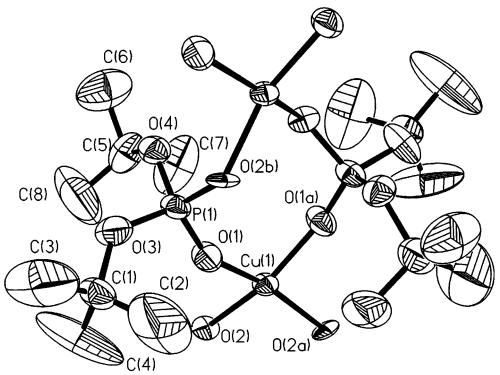

Figure 2. ORTEP (50% probability level) of the repeating unit in the structure of $[Cu(dtbp)_2]_n$ (**2**).

structure. The ORTEP diagrams of the repeating units of compounds **1**−**3** are shown in Figures 1−3. Sections of the polymeric structure using a polyhedral representation for the metal in each of these compounds are shown Figures 4−6. In all the three compounds, the dtbp acts as a bidentate bridging ligand although variations exist in the respective polymer structures. Selected bond distances and bond angles of polymers **1**−**3** are listed in Tables 2−5. A comparison of some significant structural features in these polymers is presented in Table 6.

As evident from Figures 4−6, the structure of the manganese compound **1** is analogous to Tilley's $[Zn(dtbp)_2]$ polymer,[19] while the structures of **2** and **3** represent new structural forms for polymeric dtbp complexes. Alternating triple and single di-*tert*-butyl phosphate (dtbp) bridges are found between the adjacent Mn^{2+} ions in **1** (Figure 4). Thus, the Mn^{2+} ions in **1** are tetrahedrally coordinated by four phosphate oxygen atoms. The O−M−O bond angles (103.7(1)−116.5(1)°; Table 2) around the Mn centers do not vary appreciably from the ideal tetrahedral angle. All the Mn−O distances in the molecule are almost equal (mean 2.020(3) Å) and are comparable to the Mn−O distances reported for

(23) The formation of corresponding tetrameric structures $[M_4(\mu_4\text{-O})(dtbp)_6]$ (M = Cu or Cd), however, was not observed in the absence of THF.
(24) While carboxylate (COO^-) is known to act both as a chelating and a bridging ligand, the corresponding POO^- group is not known to chelate metal ions.
(25) (a) Harrison, W. T. A.; Nenoff, T. M.; Gier, T. E.; Stucky, G. D. *Inorg. Chem.* **1992**, *31*, 5395. (b) Liu, S.-J.; Staples, R. J.; Fackler, J. P., Jr. *Polyhedron* **1992**, *18*, 2427.
(26) Du, J.-L.; Rettig, S. J.; Thompson, R. C.; Trotter, J. *Can. J. Chem.* **1991**, *69*, 277.
(27) (a) Oliver, K. W.; Rettig, S. J.; Thompson, R. C.; Trotter, J. *Can. J. Chem.* **1982**, *60*, 2017. (b) Haynes, J. S.; Oliver, K. W.; Rettig, S. J.; Thompson, R. C.; Trotter, J. *Can. J. Chem.* **1984**, *62*, 891. (c) Cini, R.; Colamarino, P.; Orioli, P. L.; Smith, L. S.; Newman, P. R.; Gillman, H. D.; Nannelli, P. *Inorg. Chem.* **1977**, *16*, 3223.
(28) Miner, V. W.; Prestegard, J. H.; Faller, J. W. *Inorg. Chem.* **1983**, *22*, 1862.
(29) Attempts to obtain X-ray diffraction quality single crystals for tetrameric manganese phosphate **4** have so far been unsuccessful.

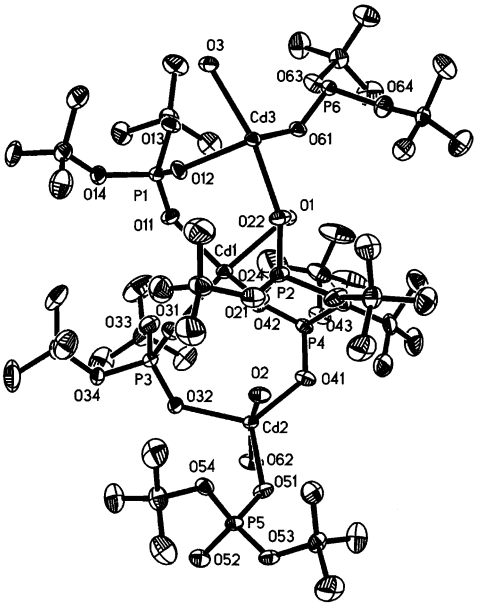

Figure 3. ORTEP (50% probability level) of the asymmetric part in the unit cell in $[Cd(dtbp)_2(H_2O)]_n$ (**3**) showing the three different unique cadmium ions.

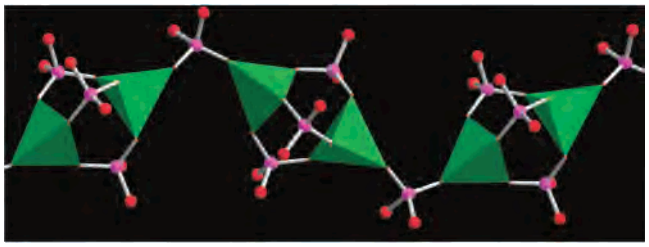

Figure 4. A section of the coordination polymer $[Mn(dtbp)_2]_n$ (**1**) with polyhedral representation for Mn^{2+} ions, also showing the alternate single and triple dtbp bridges (carbon and hydrogen atoms of the *tert*-butyl group omitted for clarity).

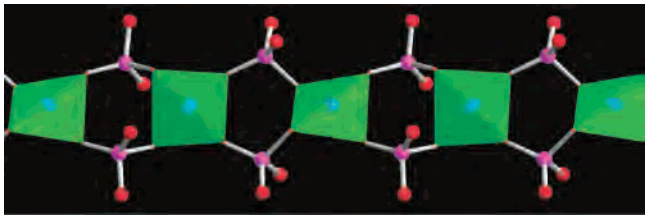

Figure 5. A section of the coordination polymer $[Cu(dtbp)_2]_n$ (**2**) with polyhedral representation for Cu^{2+} ions, also showing the double dtbp bridges (carbon and hydrogen atoms of the *tert*-butyl group omitted for clarity).

other manganese discrete and extended phosphates.[26] As expected, there are two sets of P−O distances in the molecule; while the shorter distances are associated with P−O(M) linkages (mean 1.492 Å), the longer distances correspond to P−O(C) linkages (mean 1.569(3) Å). The P−O−M angles involving single dtbp bridges are wider (150.5(2)° and 162.5(2)°) than the P−O−M angles involving the triple dtbp bridges (136.4(2)−141.9(2)°). These variations in P−O-M angles are also reflected on the Mn···Mn distances across the single and triple bridges (3.947 and 5.717 Å, respectively).

Unlike in **1**, uniform double dtbp bridges across the adjacent Cu^{2+} ions characterize the backbone of **2** (Figure

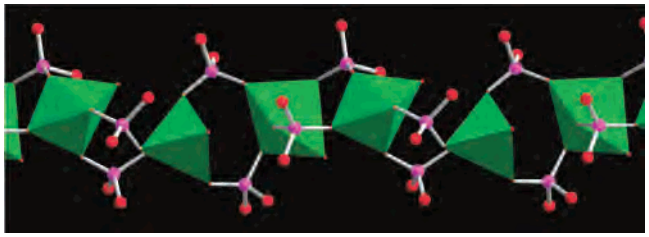

Figure 6. A section of the coordination polymer $[Cd(dtbp)_2(H_2O)]_n$ (**3**) with polyhedral representation for Cd^{2+} ions, also showing the double dtbp bridges (carbon and hydrogen atoms of the *tert*-butyl group omitted for clarity). The unconnected vertex of the cadmium polyhedron corresponds to the coordinated terminal water molecule.

Table 2. Selected Bond Lengths [Å] and Angles [deg] for Mn−Phosphate **1**

Mn(1)−O(14)	2.002(3)	Mn(2)−O(13)	2.001(3)
Mn(1)−O(2)	2.025(3)	Mn(2)−O(10)	2.009(3)
Mn(1)−O(6)	2.028(3)	Mn(2)−O(1)	2.025(3)
Mn(1)−O(9)	2.039(3)	Mn(2)−O(5)	2.031(3)
P(1)−O(1)	1.488(3)	P(2)−O(6)	1.494(3)
P(1)−O(2)	1.492(3)	P(2)−O(5)	1.496(3)
P(1)−O(4)	1.573(4)	P(2)−O(8)	1.558(3)
P(1)−O(3)	1.574(4)	P(2)−O(7)	1.572(3)
O(14)−Mn(1)−O(2)	107.3(1)	O(13)−Mn(2)−O(10)	116.4(1)
O(14)−Mn(1)−O(6)	112.5(1)	O(13)−Mn(2)−O(1)	107.0(1)
O(2)−Mn(1)−O(6)	103.7(1)	O(10)−Mn(2)−O(1)	106.5(1)
O(14)−Mn(1)−O(9)	116.3(1)	O(13)−Mn(2)−O(5)	110.0(1)
O(2)−Mn(1)−O(9)	109.0(1)	O(10)−Mn(2)−O(5)	105.6(1)
O(6)−Mn(1)−O(9)	107.3(1)	O(1)−Mn(2)−O(5)	111.4(1)
O(1)−P(1)−O(2)	117.1(2)	O(1)−P(1)−O(3)	104.0(2)
O(1)−P(1)−O(4)	112.2(2)	O(2)−P(1)−O(3)	111.2(2)
O(2)−P(1)−O(4)	104.7(2)	O(4)−P(1)−O(3)	107.4(2)
P(1)−O(1)−Mn(2)	141.9(2)	P(3)−O(9)−Mn(1)	138.9(2)
P(1)−O(2)−Mn(1)	136.5(2)	P(3)−O(10)−Mn(2)	136.4(2)
P(2)−O(5)−Mn(2)	138.2(2)	P(4)−O(13)−Mn(2)	162.5(2)
P(2)−O(6)−Mn(1)	133.6(2)	P(4a)2−O(14)−Mn(1)[a]	150.5(2)

[a] Symmetry transformation used to generate equivalent atom: a = x, $^1/_2 - y$, $^1/_2 + z$.

Table 3. Selected Bond Lengths [Å] and Angles [deg] for Cu-phosphate **2**

Cu(1)−O(1)	1.905(5)	Cu(1)−O(2)	1.932(7)
P(1)−O(1)	1.456(5)	P(1)−O(3)	1.524(6)
P(1)−O(4)	1.514(7)	P(1)−O(2b)[a]	1.556(8)
O(1)−Cu(1)−O(1a)	93.4(3)	O(4)−P(1)−O(3)	105.5(4)
O(1)−Cu(1)−O(2a)	159.9(3)	O(1)−P(1)−O(2b)	109.9(4)
O(1)−Cu(1)−O(2)	91.2(3)	O(4)−P(1)−O(2b)	105.8(4)
O(2a)−Cu(1)−O(2)	91.0(4)	O(3)−P(1)−O(2b)	104.2(4)
O(1)−P(1)−O(4)	118.1(4)	P(1)−O(1)−Cu(1)	152.6(4)
O(1)−P(1)−O(3)	112.2(3)	P(1c)−O(2)−Cu(1)	125.1(4)

[a] Symmetry transformations used to generate equivalent atoms: a = $-x + {}^3/_2$, $y + {}^1/_2$, z; b = x, $y + {}^1/_2$, $z - {}^1/_2$; c = x, $^1/_2 - y$, $^1/_2 + z$.

5). The eight-membered $Cu_2O_4P_2$ rings, which are the repeating units of this polymer, exist in an almost planar conformation.[30] There is no appreciable dihedral angle between the adjacent eight-membered $Cu_2O_4P_2$ rings, and hence, the coordination polymer can be approximated to a linear chain. The Cu···Cu separation along the polymeric chain (5.045 Å) is between the two values observed for Mn···Mn polymer **1** (vide supra). An interesting structural feature of **2** is the geometry around the central metal ion.

(30) The oxygen atom O(2) is disordered with respect two positions; when the average these positions is considered for the calculation of mean plane, the copper ion has an almost square-planar geometry.

Table 4. Selected Bond Lengths [Å] for Cd−Phosphate **3**

Cd(1)−O(11)	2.149(4)	Cd(3)−O(12)	2.207(4)
Cd(1)−O(42)	2.192(4)	Cd(3)−O(22)	2.209(4)
Cd(1)−O(21)	2.207(4)	Cd(3)−O(3)	2.337(4)
Cd(1)−O(31)	2.215(4)	P(1)−O(11)	1.493(4)
Cd(1)−O(1)	2.321(5)	P(1)−O(12)	1.494(4)
Cd(2)−O(41)	2.146(4)	P(1)−O(14)	1.566(4)
Cd(2)−O(51)	2.186(4)	P(1)−O(13)	1.595(4)
Cd(2)−O(32)	2.199(4)	P(2)−O(22)	1.476(4)
Cd(2)−O(62)	2.205(4)	P(2)−O(21)	1.499(4)
Cd(2)−O(2)	2.346(4)	P(2)−O(24)	1.581(4)
Cd(3)−O(52a)	2.170(4)	P(2)−O(23)	1.581(4)
Cd(3)−O(61)	2.206(4)		

Table 5. Selected Bond Angles [deg] for Cd−Phosphate **3**

Bond Angles around Cd(1)			
O(11)−Cd(1)−O(42)	123.9(1)	O(21)−Cd(1)−O(31)	88.5(1)
O(11)−Cd(1)−O(21)	124.6(1)	O(11)−Cd(1)−O(1)	93.4(2)
O(42)−Cd(1)−O(21)	111.2(1)	O(42)−Cd(1)−O(1)	80.4(2)
O(11)−Cd(1)−O(31)	93.6(1)	O(21)−Cd(1)−O(1)	90.3(2)
O(42)−Cd(1)−O(31)	93.0(1)	O(31)−Cd(1)−O(1)	172.3(2)
Bond Angles around Cd(2)			
O(41)−Cd(2)−O(51)	123.6(1)	O(32)−Cd(2)−O(62)	93.6(2)
O(41)−Cd(2)−O(32)	124.2(1)	O(41)−Cd(2)−O(2)	93.5(2)
O(51)−Cd(2)−O(32)	112.2(1)	O(51)−Cd(2)−O(2)	78.6(1)
O(41)−Cd(2)−O(62)	90.7(1)	O(32)−Cd(2)−O(2)	95.7(2)
O(51)−Cd(2)−O(62)	87.3(1)	O(62)−Cd(2)−O(2)	165.3(2)
Bond Angles around Cd(3)			
O(52a)−Cd(3)−O(61)[a]	126.4(1)	O(12)−Cd(3)−O(22)	89.8(1)
O(52a)−Cd(3)−O(12)	124.1(1)	O(52a)−Cd(3)−O(3)	92.8(2)
O(61)−Cd(3)−O(12)	109.3(1)	O(61)−Cd(3)−O(3)	91.6(1)
O(52a)−Cd(3)−O(22)	89.6(1)	O(12)−Cd(3)−O(3)	79.5(1)
O(61)−Cd(3)−O(22)	96.0(1)	O(22)−Cd(3)−O(3)	168.4(2)
Other Important Bond Angles			
O(11)−P(1)−O(12)	118.1(2)	O(11)−P(1)−O(13)	110.0(2)
O(11)−P(1)−O(14)	105.2(2)	O(12)−P(1)−O(13)	105.1(2)
O(12)−P(1)−O(14)	111.2(2)	O(14)−P(1)−O(13)	106.8(2)
P(1)−O(11)−Cd(1)	132.0(2)	P(4)−O(41)−Cd(2)	125.4(2)
P(1)−O(12)−Cd(3)	131.2(2)	P(4)−O(42)−Cd(1)	135.0(2)
P(2)−O(21)−Cd(1)	134.6(2)	P(5)−O(51)−Cd(2)	134.7(2)
P(2)−O(22)−Cd(3)	159.2(3)	P(5)−O(52)−Cd(3b)	129.5(2)
P(3)−O(31)−Cd(1)	130.3(3)	P(6)−O(61)−Cd(3)	132.5(2)
P(3)−O(32)−Cd(2)	127.6(2)	P(6b)−O(62)−Cd(2)	159.6(3)

[a] Symmetry transformations used to generate equivalent atoms: a = $x + 1, y, z$; b = $x - 1, y, z$.

Table 6. Key Structural Parameters in Polymers **1**−**3**

property	**1**	**2**	**3**
metal ion geometry	tetrahedral	square-planar	trigonal-bipyramidal
dtbp ligand	bidentate bridging	bidentate bridging	bidentate bridging
polymeric chain	zigzag	linear	twisted
av M−O, Å	2.02	1.89	2.19; 2.34[a]
av M···M, Å	3.95, 5.72[b]	5.05	4.50[c]
P−O−M range, deg	133.6−141.9; 150.5−162.5[b]	125.1−152.6	125.4−159.6
av *cis*-O−M−O, deg	109.4	88.8	89.9; 119.9[d]
av *trans*-O−M−O, deg		160.6	168.7

[a] Average M−O(P) and M−O(water) distances, respectively. [b] Across the triple and single dtbp bridges, resepctively. [c] 1,3-Cd···Cd distances are 8.627, 8.623, and 8.534 Å. [d] Average *cis*-O_{ax}−M−O_{eq} and *cis*-O_{eq}−M−O_{eq} angles, respectively.

Among the possible O−Cu−O angles around the tetracoordinated copper ion, one set of angles lies in the range 80.0−93.4° while the other angles fall in the range 159.9−161.3°. This observation suggests that the geometry around Cu(1) can best be described as "distorted square planar" and not "distorted or flattened tetrahedral" in view of the observed angles being closer to 90° and 180° rather than 109°. In contrast, the geometry around the Cu^{2+} ions in phosphinate polymers $[Cu(O_2PR_2)_2]_n$ (R = nC_4H_9, nC_6H_{13}) is close to a flattened tetrahedral geometry, where the bond angles lie in the range 93−150°.[27]

The structure of **3** is previously unknown in metal phosphinate, phosphonate, and phosphate chemistry (Figure 6). There are three cadmium ions in the asymmetric part of the unit cell of **3** with small differences in the coordination geometry around the metal ion. The role of the dtbp ligand in the polymeric backbone in **3** is very similar to that observed for **2**. However, the larger size of cadmium ions (compared to the smaller copper ions in **2**) results in a coordination number of five around cadmium centers. While four coordination sites around cadmium ions are occupied by four phosphate oxygen atoms, the fifth coordination site in each of the crystallographically unique cadmium ion is taken by a coordinated water molecule.

The approximate geometry around the cadmium ions is trigonal-bipyramidal (tbp). The Cd1 centers adopt a nearly ideal tbp geometry (O_{ax}−Cd1−O_{ax} = 172.3(2)°), while significant deviations are observed around Cd2 and Cd3 centers (O_{ax}−Cd2−O_{ax} = 165.3(2)°, O_{ax}−Cd3−O_{ax} = 168.4(2)°) (Table 5). The coordinated water molecule lies in the axial position in all the unique Cd^{2+} ions. In the only other structurally characterized cadmium phosphinate polymer, $[Cd(O_2P(OEt)_2)_2]$, the cadmium ions are in an octahedral geometry where the diethyl phosphate ligand is tridentate and bridges three different cadmium centers.[28]

The observed Cd−O(phosphate) distances in **3** are shorter (2.146(4)−2.215(4) Å) than the Cd−O(water) distances (2.321(5)−2.337(4) Å). These values are somewhat shorter than the similar distances in related cadmium complex $[Cd(O_2P(OEt)_2)_2]$.[28] The nonbonded Cd···Cd distances (4.443, 4.518, and 4.521 Å) observed along the polymeric chain are surprisingly shorter than those observed for copper polymer **2** (vide supra).

Thermal Decomposition Studies. To examine the utility of the one-dimensional polymers **1**−**3** as single source precursors for the preparation of metal phosphate materials, their thermal behavior has been probed (Figure 7). The TGA of **1** reveals a weight loss of 48% in the range 140−205 °C corresponding to the loss of four *iso*-butene molecules and the formation of $[Mn(O_2P(OH)_2)]$. Heating the sample up to 450 °C results in a weight loss that corresponds to the removal of two water molecules to result in $Mn(PO_3)_2$. A similar thermal behavior is found for copper polymer **2**. A more interesting thermal decomposition pattern is observed for **3**. The first weight loss of 3.3% (40−70 °C) corresponds to the loss of the coordinated water molecule. The loss of *iso*-butene corresponding to ∼41% of the initial weight occurs at 140−170 °C to produce $[Cd(O_2P(OH)_2)]$. The condensation of P−OH groups takes place in the range 180−330 °C producing $Cd(PO_3)_2$.

The results of TGA studies are also in agreement with the DSC studies. Two endothermic transitions corresponding to the loss of *iso*-butene and water were observed for

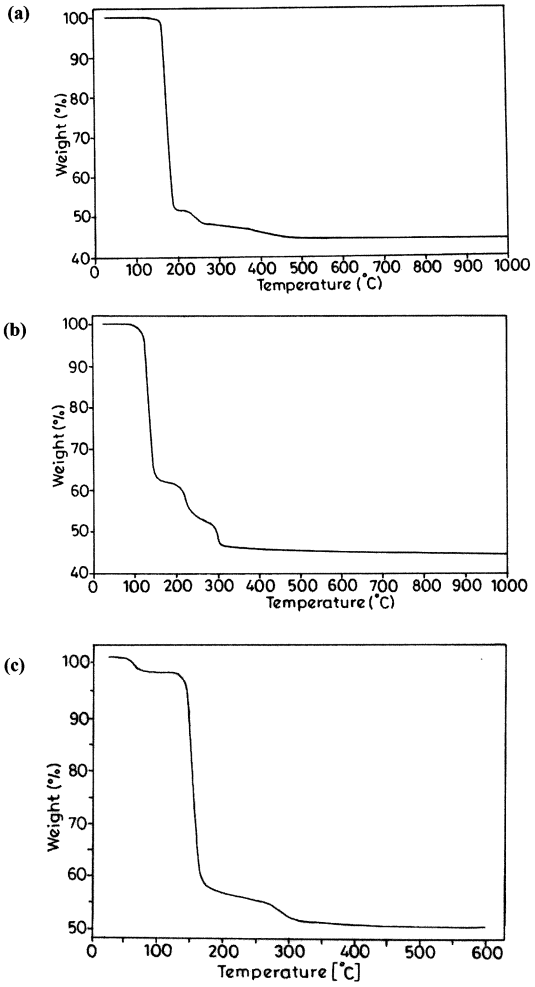

Figure 7. TGA curves for the coordination polymers for (a) $[Mn(dtbp)_2]_n$ (**1**), (b) $[Cu(dtbp)_2]_n$ (**2**), and (c) $[Cd(dtbp)_2(H_2O)]_n$ (**3**).

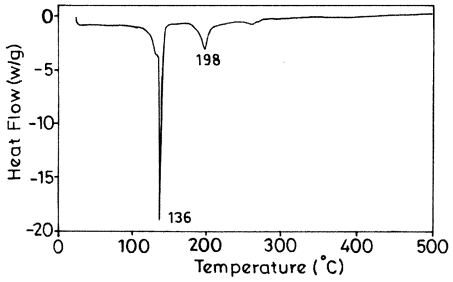

Figure 8. DSC curve for the coordination polymer $[Cu(dtbp)_2]_n$ (**2**).

compounds **1** and **2**. For example, the DSC curve depicting copper polymer **2** in Figure 8 reveals these transitions occurring at 136 and 198 °C, respectively.

To further substantiate these findings, bulk decomposition of polymers **1**−**3** has been carried out. Because in all three cases the decomposition is complete before 600 °C to produce the final material, the bulk samples of **1**−**3** were heated in a furnace at 200, 300, 350, 400, 500, and 600 °C for 4 h in the flow of air. The resultant solid material in each case was characterized with the aid of powder XRD and IR spectroscopy. Because the results obtained for **1**−**3** are very similar, only the details of studies on **3** are described herein. Figures 9 and 10 depict the PXRD patterns and IR

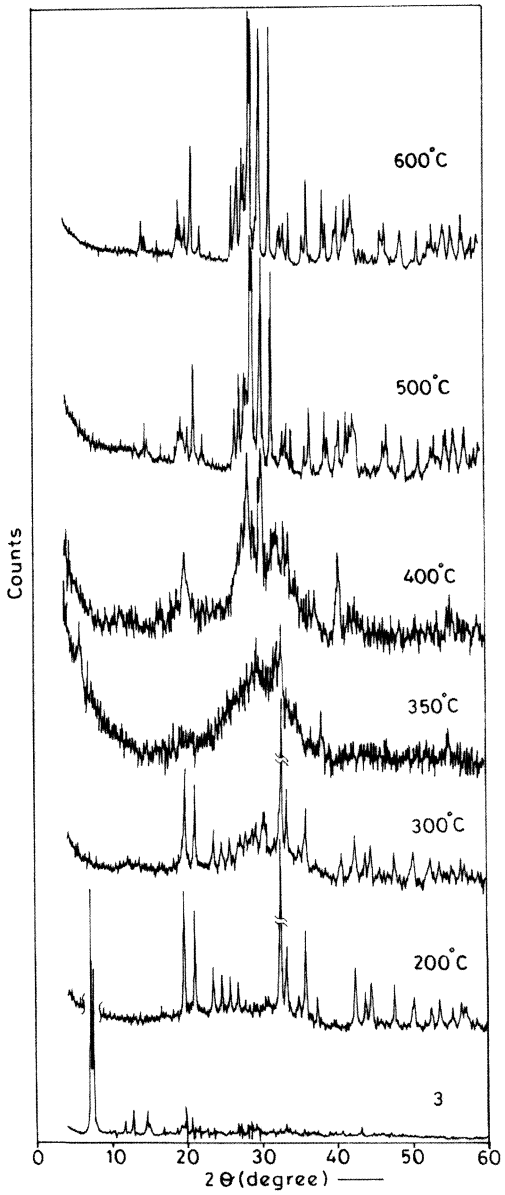

Figure 9. Powder X-ray diffraction pattern for as-synthesized $[Cd(dtbp)_2(H_2O)]_n$ (**3**) and the samples heated at various temperatures.

spectra of thermal decomposition products of **3** heated at various temperatures along with those of the analytically pure crystalline sample of **3** itself. Heating **3** at 200 °C leads to a crystalline material which corresponds to the molecular formula $[Cd(O_2P(OH)_2)]$. Raising the temperature to 350 °C results in the collapse of the crystalline structure because of the release of water from the condensation of P−OH groups to produce $Cd(PO_3)_2$. The XRD pattern shows the highly amorphous nature of the material. Heating the sample further at 500 °C results in the sharpening of the peaks and formation of fully crystalline $Cd(PO_3)_2$ material.[31] The IR spectra of the samples shown in Figure 10 also clearly support the findings of thermal analysis. The absorptions corresponding to C−H vibrations of *tert*-butyl groups almost disappear in the sample heated at 200 °C. Decomposition products of compounds **1** and **2** also show very similar XRD and IR

(31) See JCPDF 210122 for diffraction data of $Cd(PO_3)_2$.

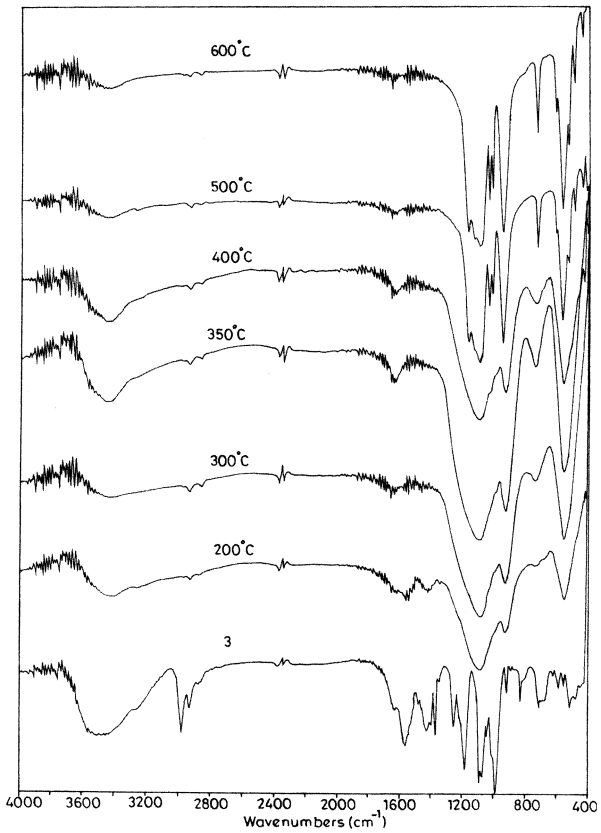

Figure 10. IR spectra for as-synthesized $[Cd(dtbp)_2(H_2O)]_n$ (**3**) and the samples heated at various temperatures.

spectral behavior. The most significant observation during the described process is the formation of the amorphous metaphosphate $Cd(PO_3)_2$ from **3** at temperatures as low as 350 °C. This is the lowest temperature we have observed thus far for the phosphate material formation from a metal-dtbp precursor complex.

The broad peaks observed in the XRD pattern of decomposition products (e.g., Figure 9; sample heated at 350 °C) prompted us to carry out N_2 adsorption studies on these samples in order to explore their surface properties. The results of these studies summarized in Table 7, however, show that these samples are not porous. The BET surface area of the sample of **3** heated at 350 °C, for example, is 18.7 m^2/g. The somewhat large mean pore diameter obtained for these samples probably is indicative of the distance between two particles rather than the diameters of actual pores. This observation indicates that the solid state decomposition procedure employed herein results only in larger particles although one can expect an entirely different decomposition behavior in solution, especially from a high boiling hydrocarbon. Experiments in this direction are currently underway.

Table 7. Results of N_2 Adsorption Experiments on Thermal Decomposition Products of **3**

entry	decomposition temperature[a]	BET surface area (m^2/g)	pore volume (cc/g)	pore diameter (Å)
1	200	19.0	0.39	814
2	300	12.2	0.35	1143
3	350	18.7	0.43	981
4	400	12.4	0.32	1015
5	500	7.6	0.12	618
6	600	6.4	0.16	1017

[a] See Experimental Section for details.

Conclusion

A simple and facile metal-organic precursor route for the synthesis of transition metal metaphosphate materials at low temperatures has been demonstrated. The formation of polymeric phosphates over the other types of metal phosphates is facilitated by the addition of THF or a mild base during the course of the reaction. The synthetic strategy we have employed herein has several advantages over the earlier methods described in the literature for the preparation of metal phosphate precursor complexes: for example, (a) use of cheaper and commercially available metal acetates as starting materials, (b) the use of less stringent reaction conditions without employing any anaerobic conditions, and (c) the use of solvents such as methanol. The metal acetate route should in principle be applicable to the synthesis of other transition metal or main group phosphates. The presence of a large number of hydrolyzable and thermally labile *t*BuO groups on the surface of polymers **1**−**3** can be exploited for the preparation of metal-containing silicophosphate materials (SMPO) under appropriate conditions in the presence of a suitable silicon source.

Acknowledgment. This work was supported by DST, New Delhi. R.M. also thanks the DST for the award of Swarnajayanti Fellowship. We thank the RSIC- and DST-funded Single Crystal X-ray Diffractometer Facility, IIT-Bombay, for the spectral, thermal, and diffraction data.

Supporting Information Available: Crystallographic data for **1**−**3** in CIF format. This material is available free of charge at http://pubs.acs.org.

IC0259787